






Article

Study of the Carbochlorination Process with CaCl_2 and Water Leaching for the Extraction of Lithium from Spent Lithium-Ion Batteries

Yarivith C. González ^{1,2,*} , Lorena Alcaraz ^{3,*} , Francisco J. Alguacil ³ , Jorge González ^{1,2}, Lucía Barbosa ^{1,2}  and Félix A. López ³ 

¹ Instituto de Investigación en Tecnología Química (INTEQUI-CONICET), A. Brown 1455, San Luis D5700, Argentina

² Facultad de Química Bioquímica y Farmacia (FQBF), UNSL, Ejército de los Andes 950, San Luis D5700, Argentina

³ Centro Nacional de Investigaciones Metalúrgicas (CENIM), Consejo Superior de Investigaciones Científicas (CSIC), Avda. Gregorio del Amo 8, 28040 Madrid, España

* Correspondence: yarithgon11@gmail.com (Y.C.G.); alcaraz@cenim.csic.es (L.A.); Tel.: +34-911992202 (L.A.)

Abstract: The abundant use of lithium-ion batteries (LIBs) in a wide variety of electric devices and vehicles will generate a large number of depleted batteries, which contain several valuable metals, such as Li, Co, Mn, and Ni, present in the structure of the cathode material (LiMO_2). The present work investigates the extraction of lithium, as lithium chloride, from spent LIBs by carbochlorination roasting. The starting samples consisted of a mixture of cathode and anode materials from different spent LIBs known as black mass. Calcium chloride was used as a chlorinating agent, and carbon black was used as a reducing agent. The black mass, calcium chloride, and carbon black were mixed in 50:20:30 *w/w* % proportions. Non-isothermal thermogravimetric tests up to 850 °C and isothermal tests at 350, 500, and 700 °C were carried out in an inert atmosphere. It was observed that the carbochlorination reaction starts at 500 °C. An extraction percentage of 99% was attained through carbochlorination at 700 °C. The characterization results indicate that CaCO_3 , Ni, and Co and, to a lesser extent, CoO, NiO, and MnO_2 are present in the roasted sample after the processes of washing, filtering, and drying.

Keywords: carbochlorination; spent lithium-ion batteries; circular economy; recycle; LiCl



Citation: González, Y.C.; Alcaraz, L.; Alguacil, F.J.; González, J.; Barbosa, L.; López, F.A. Study of the Carbochlorination Process with CaCl_2 and Water Leaching for the Extraction of Lithium from Spent Lithium-Ion Batteries. *Batteries* **2023**, *9*, 12. <https://doi.org/10.3390/batteries9010012>

Academic Editor: Carlos Ziebert

Received: 21 October 2022

Revised: 21 December 2022

Accepted: 22 December 2022

Published: 25 December 2022



Copyright: © 2022 by the authors. Licensee MDPI, Basel, Switzerland. This article is an open access article distributed under the terms and conditions of the Creative Commons Attribution (CC BY) license (<https://creativecommons.org/licenses/by/4.0/>).

1. Introduction

Lithium-ion batteries (LIBs) are widely used in portable devices due to their high energy density to weight ratio, reduced memory effect, and a significant number of charge/discharge cycles [1]. In addition, LIBs are being increasingly used in electromobility technologies for transportation and the alternative energy industry [2,3]. Thus, the global lithium market is expected to increase by around 87% by 2025 due to the anticipated expansion of LIBs for their large applications. The increase in demand for LIBs causes some concern about the supply of the primary resources needed to manufacture new batteries in the medium term [4]. Thus, their recycling is of the utmost interest.

In general, LIBs consist of a cathode, an anode, and a polymeric separator impregnated with an electrolyte that enables the ionic conduction of lithium ions. The active material used in the cathode can vary depending on the manufacturer [3]. The most common compounds of the cathode material are LiCoO_2 , LiMn_2O_4 , and LiFePO_4 , among others [5]. On the other hand, the active material commonly used in the anode is graphite [6,7].

Because of the limited lifetime of LIBs, 11 million tons of spent batteries are estimated to be produced by 2030 [7,8]. Recently, a report by the United Nations University revealed that a high percentage of electronic waste, including spent LIBs, is highly polluting because it often contains Li, Co, Mn, and Ni, among others. It is predicted that 80 GWh of LIBs will

be discarded as waste by 2025 [9]. This figure is equivalent to the global battery market of 2017, which corresponds to 64,000 tons of Li and 18,000 tons of Co. Therefore, the proper management of the final disposal of spent LIBs is of great concern.

Recycling spent batteries is an interesting alternative to deal with both the supply issues of manufacturing new batteries and the polluting effects of discarded batteries [10]. The recycling of discarded LIBs focuses mainly on the recovery of strategic metals: lithium and transition metals, such as nickel, manganese, and cobalt. These recovered metals could be reused in the manufacture of new battery electrodes [11,12]. Additionally, the recovered lithium could be used in many other applications, including glass and ceramics, lubricants and greases, aluminum production, and air treatment. Even in the medical field, lithium is applied in various treatments: bipolar disorder, depression, dental, and headaches [13]. The recovery of cobalt and nickel from spent LIBs could also be beneficial because the extraction of these metals from primary resources is expensive and highly polluting. The main reserves are found in the Democratic Republic of Congo. Much of the extraction work is done by hand, posing a risk to the environment and human health [14]. Therefore, recycling spent batteries may contribute to the circular economy [15–17].

Many studies have been conducted focusing on the recovery of metals from spent LIBs by applying different methods. Hydrometallurgy and pyrometallurgy are the most typical methods [18–20]. Hydrometallurgy uses different leaching agents, including hydrochloric acid (HCl), nitric acid (HNO₃), and phosphoric acid (H₃PO₄), to extract the targeted metals [21–23]. Whereas pyrometallurgy uses heat to induce a chemical change in the components of the LIBs to extract the metals of interest.

Carbothermic reduction has become an important pyrometallurgical method [24–26]. This method implies the use of a carbonaceous material fulfilling the function of a reducing agent. The metals are directly recovered as Li₂CO₃, CoO, and MnO. Temperatures as low as 550 °C were found to be optimum for metal recovery using carbon black (CB) as the reducing agent [18]. Chlorination roasting was also studied as an alternative pyrometallurgical method to recover metals such as LiCl, CoCl₂, MnCl₂, and NiCl₂. An extraction yield as high as 100% was reached at 900 °C and 90 min using chlorine as chlorinating agent [27]. The main key to these processes is to break the chemical bonds of the cathode material with the general formula LiMO₂ (usually M = Co or Ni). Thus, Li and M can be converted into two different species that can be separated by precipitation, phase separation, solvent extraction, or in the form of oxides according to the applied method [1]. Herein, we propose an innovative carbochlorination process as an alternative method to recover metals from spent LIBs by combining the important aspects of carbothermal reduction and chlorination roasting.

Carbochlorination consists of the chlorination reaction leading to metallic chlorides in the presence of a chlorinating agent and a carbonaceous material in a dry atmosphere [28]. It is favored over direct chlorination regarding thermodynamic and kinetic aspects, which in turn results in an important reduction in the reaction temperature. The carbonaceous material fulfills a dual function: as an oxygen acceptor favoring metal reduction and as a catalyst generating and capturing active chlorine species [29]. Regarding the chlorinating agent, various compounds, including gaseous chlorine (Cl₂), HCl, CCl₄, MgCl₂, and CaCl₂, were used depending on the metal or sample to be chlorinated [30]. Calcium chloride (CaCl₂) is a very low-cost reagent and can be acquired as a by-product of the Solvay process. This chloride has already been used to extract lithium, as lithium chloride, from β-spodumene [31]. Previous investigations have reported that the chlorination roasting-water leaching process can be efficient in extracting valuable metals from spent lithium-ion batteries [32,33]. Calcium chloride has also been used to extract lithium by the chlorination roasting of a slag, simulated as obtained from pyrometallurgical recycling, consisting of pre-heating, plastic pyrolyzing, and smelting, along with reducing, reaching a lithium extraction efficiency of 90.58% at 800 °C for 60 min [34].

In the present work, a carbochlorination method using CaCl_2 as a chlorinating agent and carbon black (CB) as a reducing agent is researched to recover metals from spent LIBs. Different experimental conditions are evaluated to establish an efficient process.

2. Materials and Methods

The starting materials were three samples called black mass samples (BMs). The source of one BM was smartphones, and the source of the other two BMs was electric/hybrid vehicles. The BMs from smartphones were called SBM, and those from electric/hybrid vehicles were called VBM-1 and VBM-2. Calcium chloride with 99% purity (Panreac Applichem) was used as the chlorinating agent. In addition, commercial carbon black was used as the reducing agent. Carbon black and calcium chloride were added to each original black mass sample to prepare a mixture using a mortar. The proportions of the mixture were 50, 20, and 30 *w/w* % of black mass, calcium chloride, and carbon black, respectively. The proportions of CaCl_2 and carbon black were calculated based on the percentage of lithium present in the BM. For comparison purposes, a mixture of black mass and calcium chloride was also prepared in 50/50 *w/w* % proportions. All carbochlorination experiments were carried out in a nitrogen atmosphere of 99.99% *v/v*.

2.1. X-ray Diffraction (XRD)

The structural characterization of the starting black mass samples and the products obtained after the reaction were made by X-ray diffraction (XRD). Except for the crystallized soluble products (SPs), XRD measurements were collected on a Rigaku D-Max-III C diffractometer operated at 30 kV and 20 mA, using the $K\alpha$ radiation of Cr and the filter of V. The structural characterization of the crystallized soluble products (SPs) was evaluated by XRD using a PANalytical multi-purpose diffractometer model X'Pert PRO MPD, which is equipped with a high-temperature chamber for use with temperature diffraction measurements, with a Cu anode (Cu $K\alpha$ radiation). The XRD measurements at 70 °C were obtained using a heating ramp of 10 °C min^{-1} .

2.2. Atomic Absorption Spectroscopy (AAS)

Metal concentrations in aqueous solutions were analyzed by atomic absorption spectroscopy (AAS) using a Perkin Elmer 1100B spectrophotometer. Previously, each BM was dissolved with aqua regia solution and was moderately heated for several hours. Then, the final solution was filtered, and the obtained insoluble solid was dried to calculate the graphite carbon content in each sample. The determination of the percentage of carbon in the initial samples was carried out using the combustion technique in an induction furnace and infrared absorption detection.

2.3. Scanning Electron Microscopy (SEM)

The morphology of all the samples was analyzed by field emission scanning electron microscopy (FE-SEM) using a LEO 1450 VP microscope equipped with an EDAX Genesis 2000 energy-dispersive spectrometer and a Hitachi S-4800 equipped with an energy-dispersive X-ray microanalyzer (EDX). For SEM observations, the powder samples were placed on an adhesive conductive carbon disk. In the case of the NS-samples, the powders were embedded into a conductive resin due to the magnetism of the products.

2.4. Thermogravimetric Analysis (TGA) and Differential Thermogravimetric Analysis (DTG)

The non-isothermal calcination tests were conducted in a thermogravimetric system suitable for working in corrosive and non-corrosive atmospheres designed in our laboratory [35]. Isothermal carbochlorination tests were carried out in a high alumina tubular reactor, with a circulating-flow system. The sample was contained in a high alumina crucible that was then placed inside the reactor at the required temperature and for the specific working time.

3. Experimental Procedure

3.1. Non-Isothermal Experiments

The BM/CaCl₂ and BM/CaCl₂/CB mixtures were analyzed by thermogravimetric analysis (TGA). The mixture samples were studied by thermogravimetric analysis (TGA). In this step, 250 mg of each sample was put in a large alumina crucible. The crucible containing the sample was placed inside a tubular reactor. Immediately, the heating program of 5 °C/min was run until it reached 850 °C. A nitrogen current circulated at 20 mL min⁻¹ during the whole heating period. After the experiment, the sample was cooled down and withdrawn from the reactor for further analysis.

3.2. Isothermal Experiments

Both BM/CaCl₂ and BM/CaCl₂/carbon black mixtures were heated at isothermal conditions. Temperatures of 350 °C, 500 °C, and 700 °C were investigated, using a different sample for each temperature. These temperatures were selected by analyzing the derivative of the TGA curve of the BM/CaCl₂ and BM/CaCl₂/carbon black mixtures. The sample was put in a large alumina crucible that was then placed inside the tubular reactor, with a through-flow system circulating 20 mL·min⁻¹ of nitrogen. The heating program was run at 5 °C·min⁻¹ until it reached the working temperature, and then, the temperature was held constant for 60 min. After the reaction time was fulfilled, the crucible containing the calcined sample was removed from the reactor and cooled. Subsequently, the calcined sample was washed with distilled water at 70 °C. After washing, the slurry obtained was filtered. The filtrate solution was analyzed by AAS to measure lithium concentration. Then, the filtrate solution and the wet solid retained on the filter were left in an oven until dry. The crystallized solids from the filtrate were identified as soluble products (SPs), and the dried solids were identified as non-soluble products (NSP). SP and NSP samples were characterized by XRD and SEM-EDS.

Lithium extraction was calculated using Equation (1):

$$X = \frac{m_f}{m_i} \cdot 100 \quad (1)$$

where X is the lithium extraction as a percentage, m_i is the initial mass of Li in the black mass sample, determined using the concentration of Li in the original black mass sample, and m_f is the mass of Li in the soluble products, determined using the concentration of Li in the filtrate solution obtained after washing the calcined samples.

4. Results and Discussion

4.1. Characterization of the Initial Black Mass Samples

After the leaching of the BM with aqua regia, a black solid remained insoluble. This residue could be graphite, proceeding from the anode material. Table 1 shows the metal and carbon concentrations measured by AAS and combustion, respectively. The calculated total carbon content was around 30–33% for the three samples.

Table 1. Composition of metals and carbon of the black mass samples (weight percentage %).

Sample	Li	Co	Mn	Ni	Cu	C
SBM 1	4.5	30	4.30	0.90	0.30	33.3
VBM-1	3.11	5.62	10.1	11.2	2.2	32
VBM-2	5.2	3.2	n.d.	41.2	1.2	30.9

n.d.—not detected.

The XRD patterns for SBM, VBM-1, and VBM-2 are shown in Figure 1. Diffraction maxima were found that can be attributed to the phases of LiCoO₂ for SBM, LiNi_{0.5}Mn_{1.5}O₄ for VM-1, and, to a lesser extent, LiNiO₂ for VM-2. Several reflection maxima corresponding to the carbon graphite phase were detected in the three samples SBM, VBM-1, and VBM-2. Thus, the high carbon content in black mass samples is related to crystalline carbon graphite.

This result agrees well with the chemical composition of the initial samples. Figure 2 shows SEM micrographs and EDS spectra from particles of each black mass sample. VBM-1 and VBM-2 samples are made up of agglomerates of rounded primary particles. The micrograph of the SBM sample exhibits particles without a regular form having a smooth surface and sharp edges. Regarding the EDS results, the elements detected are as follows: C, O, Ni, Al, Mn, and Co in VBM-1; C, O, Al, Co, and Ni in VBM-2; and C, O, Co, and Si in SBM.

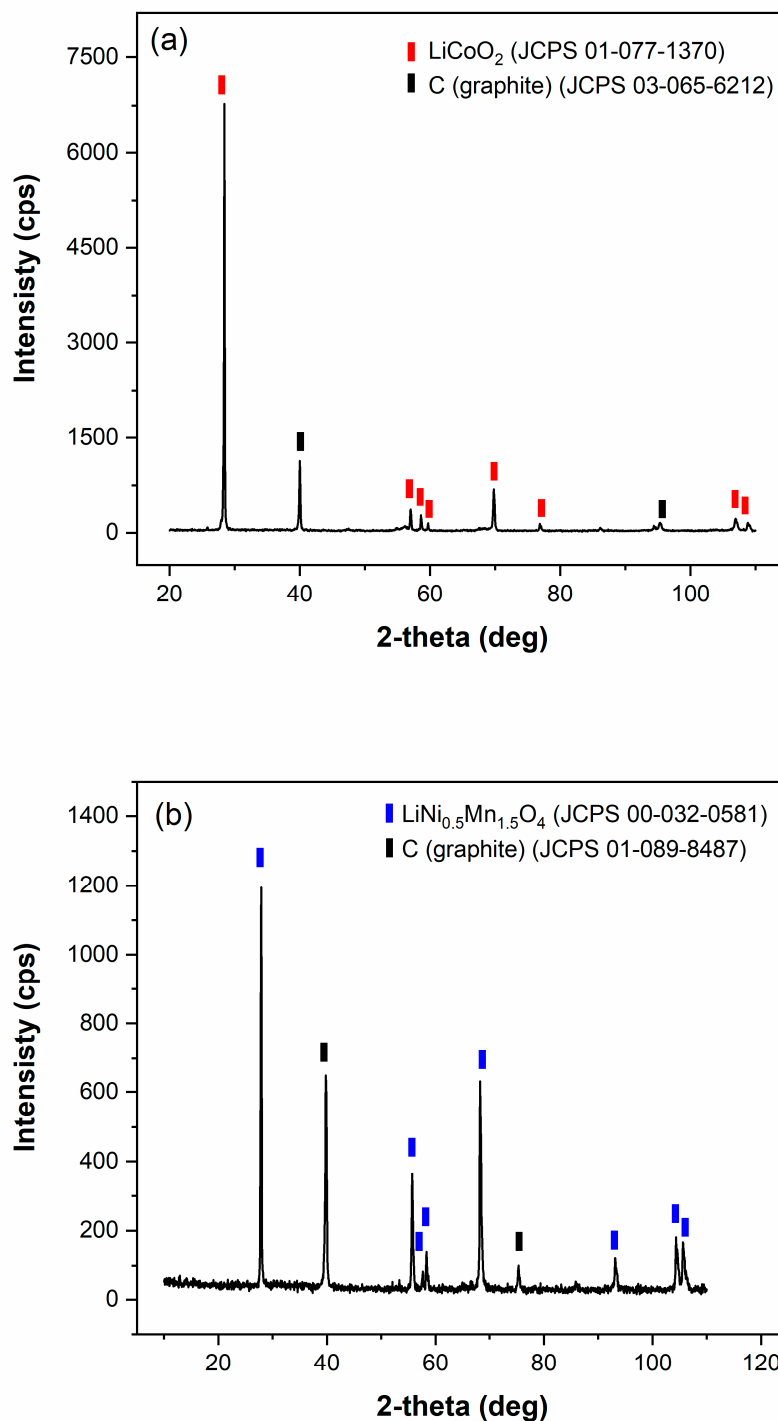


Figure 1. Cont.

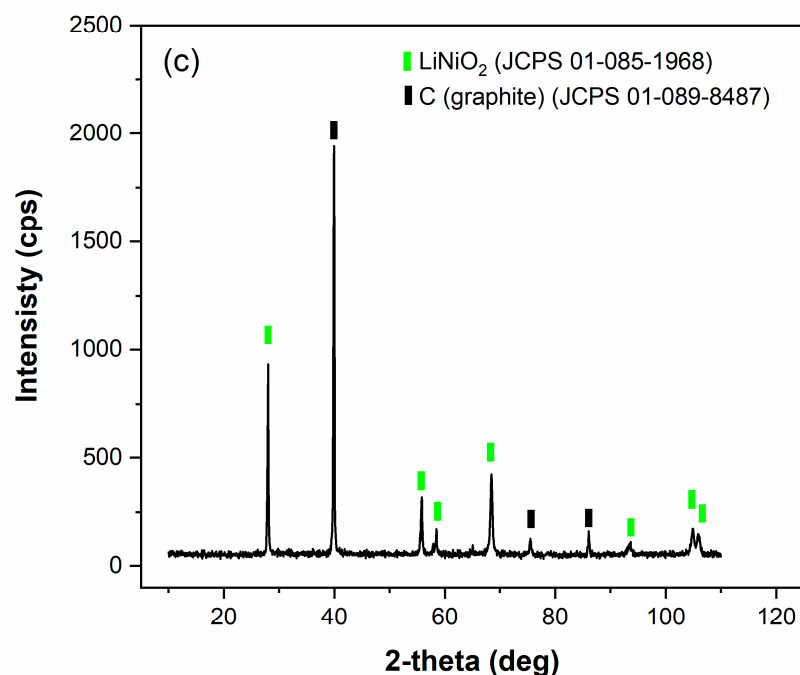


Figure 1. Diffractograms of the black mass samples from spent LIBs: (a) SBM, (b) VBM-1, and (c) VBM-2.

4.2. Non-Isothermal Experiments

Figure 3 shows the thermograms obtained after the non-isothermal experiment. The first mass loss can be distinguished between 40 and 210 °C, which can be associated with loss of moisture for all samples. Between 212 and 695 °C, a small mass loss of approximately 3%, 7%, and 8% for SBM, VBM-1, and VBM-2, respectively, can be observed. This mass loss can be attributed to the volatilization of impurities present in the original black mass sample. These impurities can be associated with the binders, the electrolytic and organic solvents, and the other contaminants acquired in the initial pretreatment and disassembly process. Between 700 and 850 °C, a marked mass loss zone can be detected: 20%, 24%, and 32% for SBM, VBM-1, and VBM-2, respectively. This last mass loss could be related to the release of CO₂ as a product of the reduction of cobalt, nickel, and manganese and the release of CO₂. It is expected that during the heat treatment, lithium chloride is produced. Thus, the mass loss detected between 700 and 800 °C could also be attributed, in part, to either the volatilization of volatile lithium chloride or the reaction of lithium chloride with the crucible made up of alumina [36].

4.3. Isothermal Experiments

Table 2 shows the mass losses of BM/CaCl₂ and BM/CaCl₂/carbon black mixtures after being heat-treated at isothermal conditions. These mass losses coincide with those shown in Figure 3, being associated with the loss of impurity in the sample. At 500 °C, the increase in mass loss is associated with the release of CO₂ by the carbon effect and, finally, at 700 °C, with the reduction of Ni and Co to the metallic state.

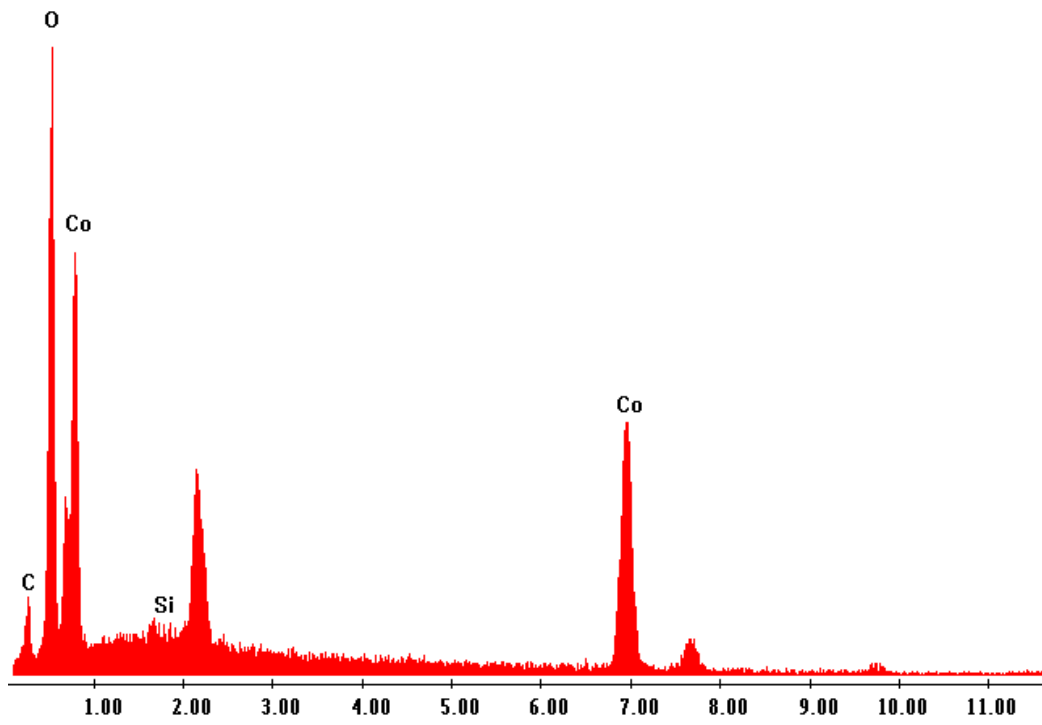
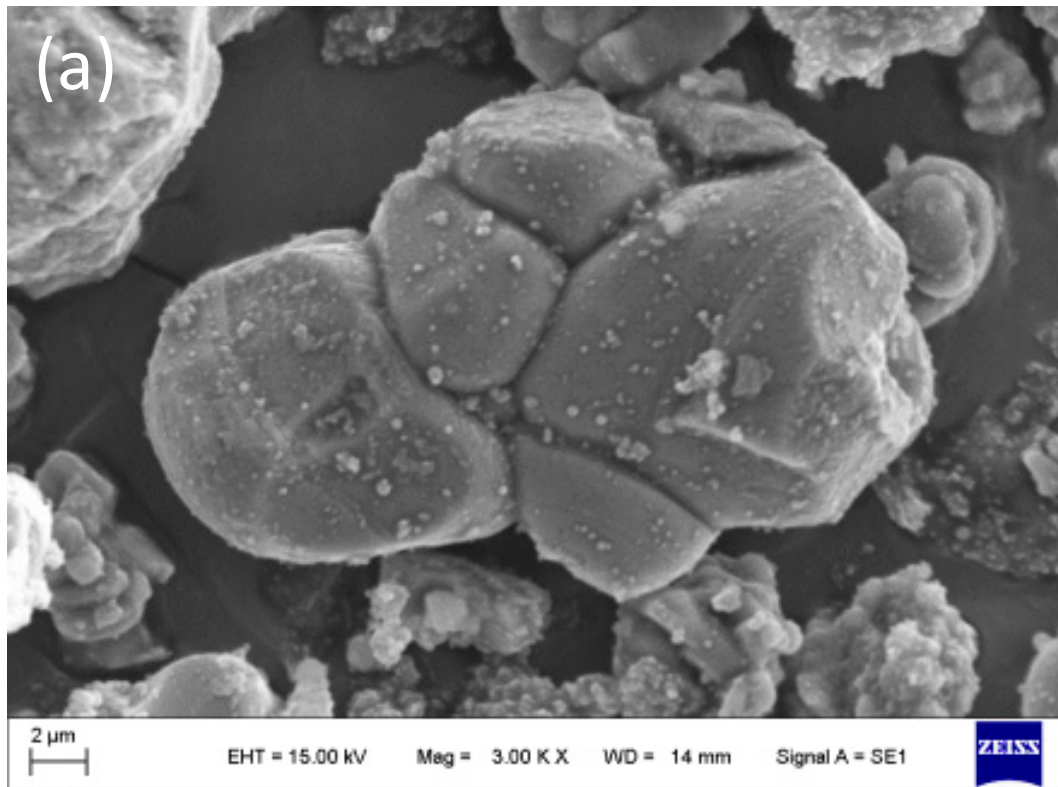


Figure 2. Cont.

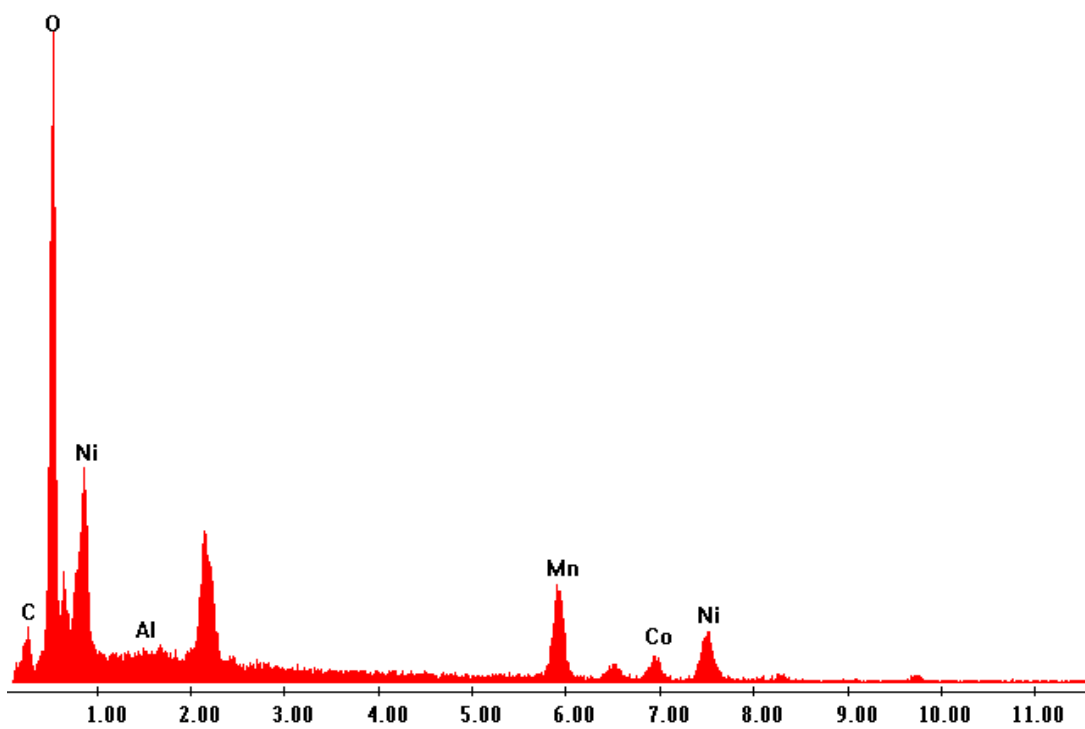
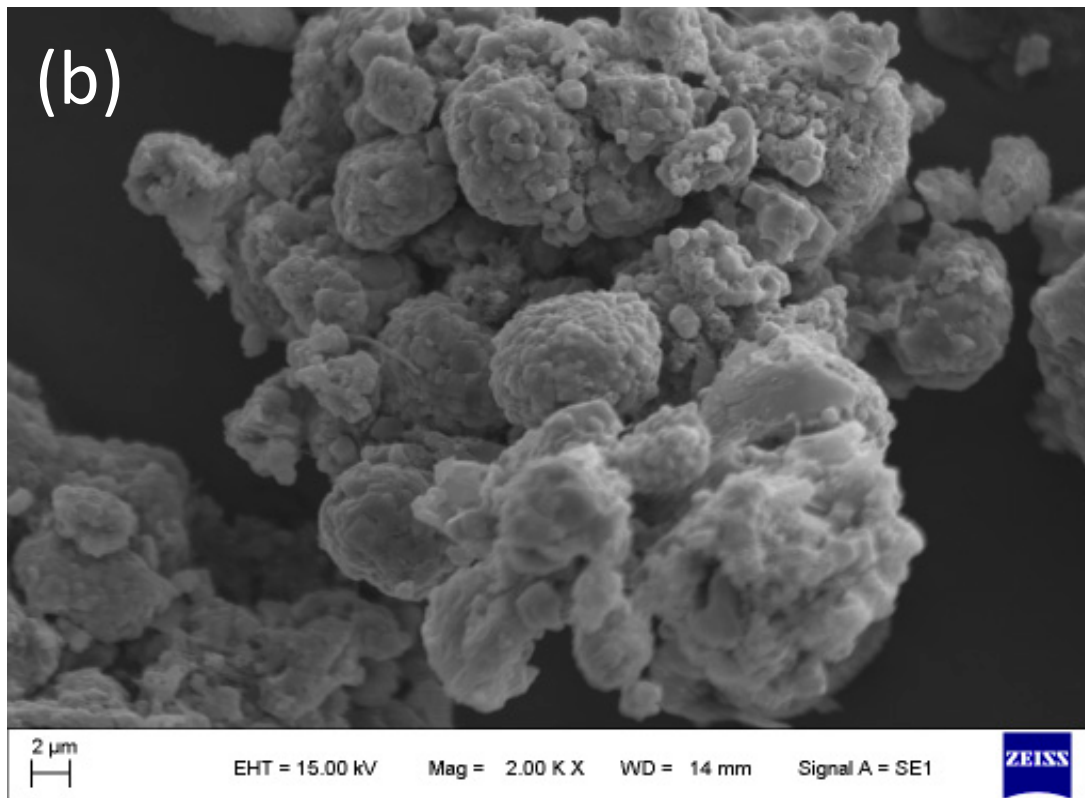


Figure 2. Cont.

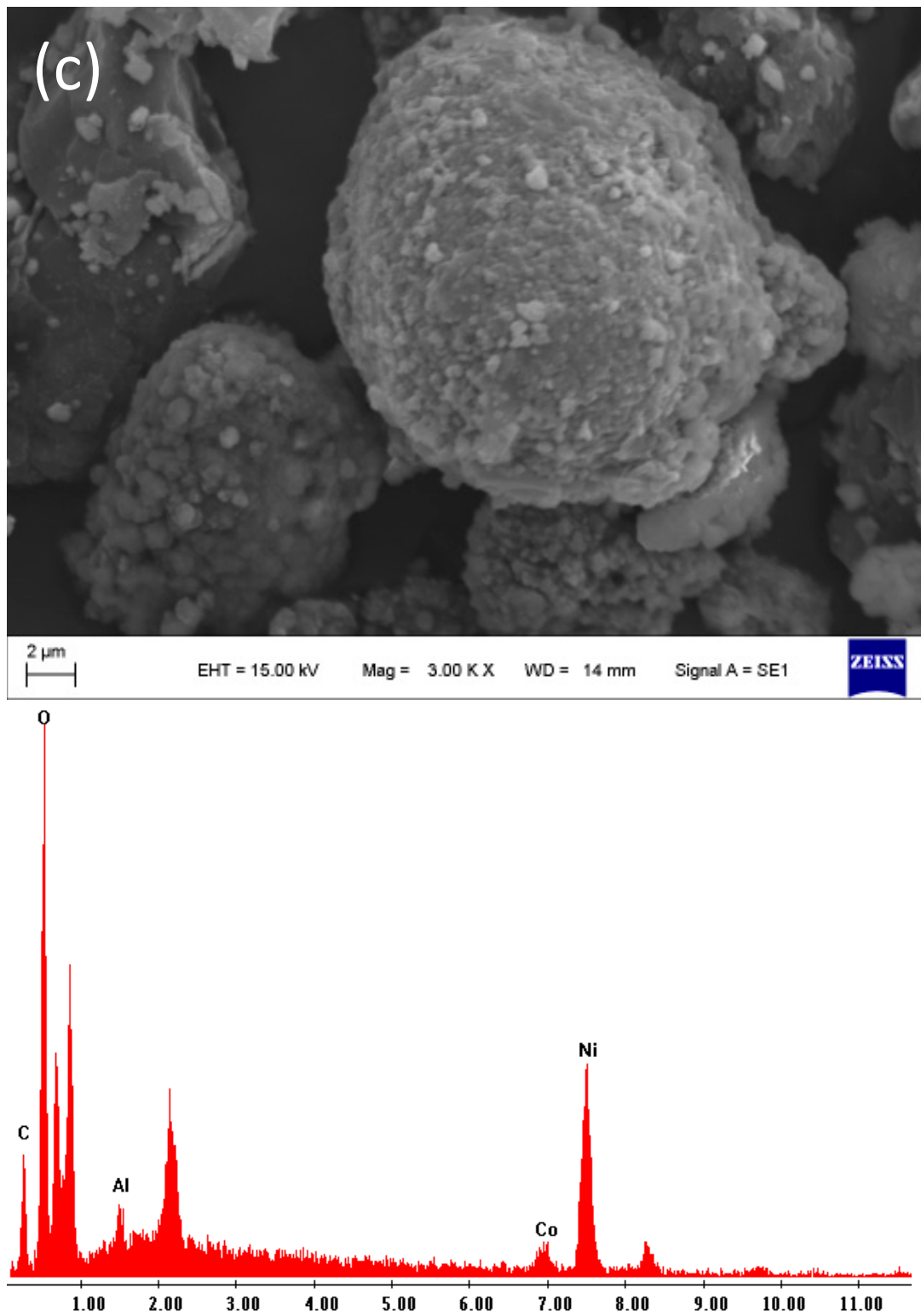


Figure 2. SEM micrographs and EDS spectra from particles of each black mass sample, (a) SBM, (b) VBM-1, and (c) VBM-2.

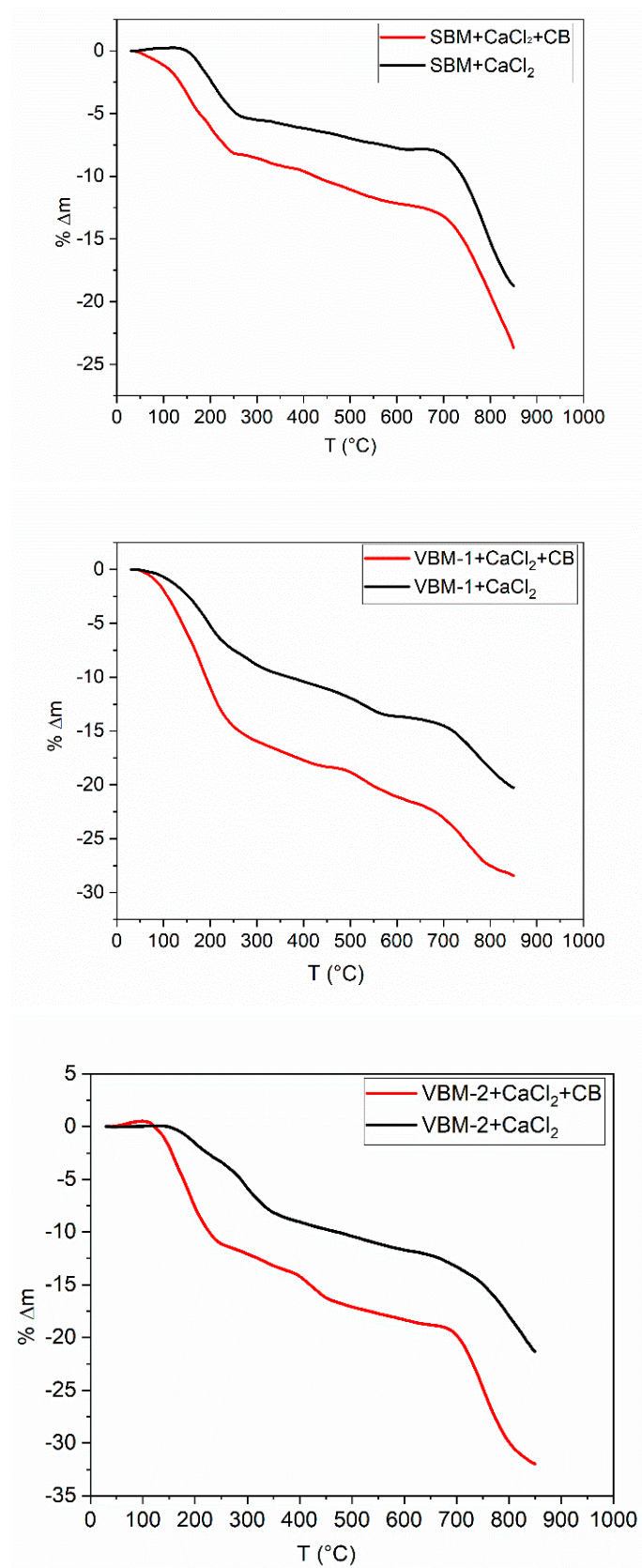
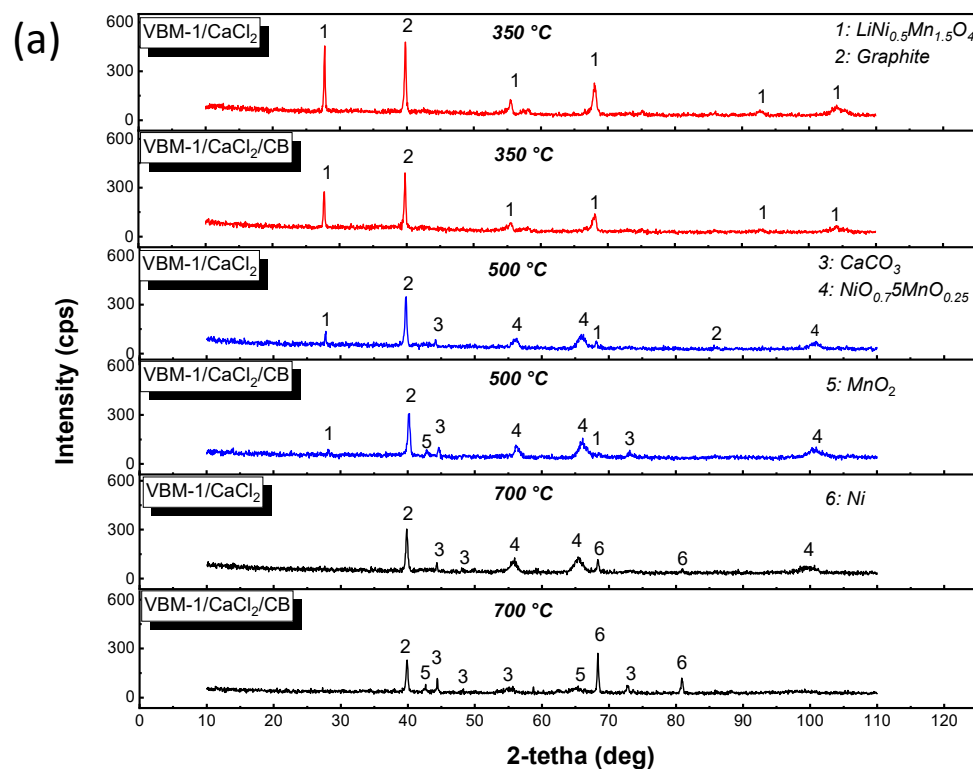


Figure 3. TGA of the BM/CaCl₂ and BM/CaCl₂/carbon black mixture in N₂ stream.

Table 2. Mass loss of the mixtures calcined at isothermal conditions.

Temperature (°C)	BM/CaCl ₂	Δm (%)	BM/CaCl ₂ /Carbon Black	Δm (%)
350	VBM-1	7	VBM-1	24
	VBM-2	12	VBM-2	20
	SBM	4	SBM	27
500	VBM-1	10	VBM-1	27
	VBM-2	14	VBM-2	25
	SBM	6	SBM	27
700	VBM-1	12	VBM-1	30
	VBM-2	15	VBM-2	30
	SBM	7	SBM	31

Figure 4 shows the XRD patterns of the NSP samples obtained after each isothermal calcination of both mixtures BM/CaCl₂ and BM/CaCl₂/CB. Figure 4a–c show the results of VBM-1, VBM-2, and SBM, respectively. Regarding VBM-1, at 350 °C, the peaks of the LiNi_{0.5}Mn_{1.5}O₄ phase found in the original sample are still present in the XRD pattern of the NSP sample. At 500 °C, the peak intensity of the LiMn_{0.5}Ni_{1.5}O₂ phase decreases significantly, but the decrease is more noticeable in the case of the VBM-1/CaCl₂/CB system. We can infer that at 500 °C, LiMn_{0.5}Ni_{1.5}O₂ starts to react with CaCl₂, and the reaction is favored when CB is present because peaks of CaCO₃ and mixed Ni and Mn oxide start to become noticeable. At 700 °C, the LiMn_{0.5}Ni_{1.5}O₂ is no longer detected in either case. In the case of the VBM-1/CaCl₂ system, peaks characteristic of mixed Ni and Mn oxide and CaCO₃ are predominantly observed. In the case of the VBM-1/CaCl₂/CB system, very intense peaks corresponding to metallic Ni can be observed. Peaks of CaCO₃ and MnO₂ are also identified as reaction products.

**Figure 4.** Cont.

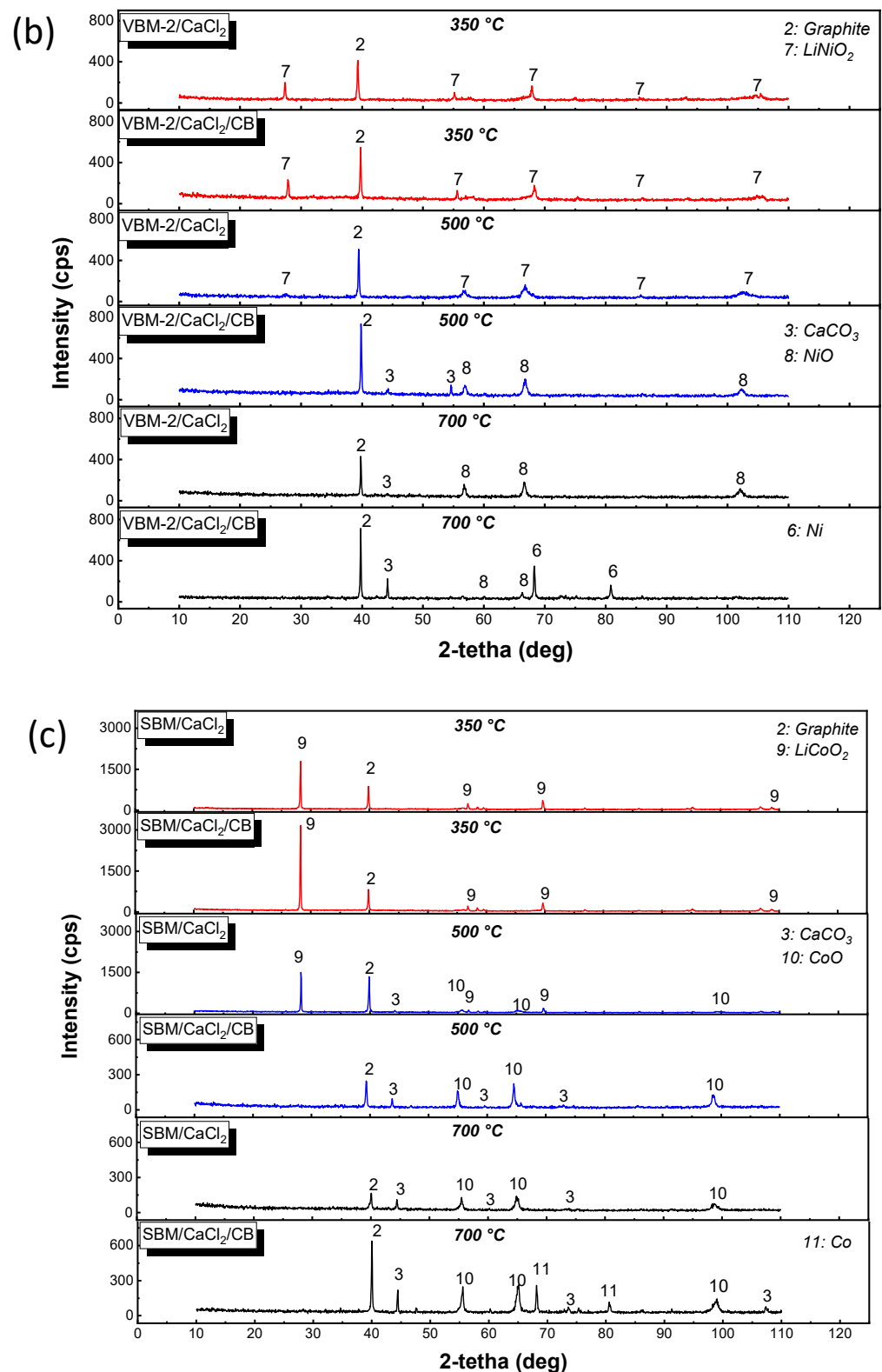


Figure 4. XRD patterns of the NSP samples obtained after the isothermal calcination of both mixtures BM/CaCl₂ and BM/CaCl₂/CB: (a) VBM-1, (b) VBM-2, and (c) SBM.

With respect to VBM-2, at 350 °C, the peaks of the LiNiO₂ phase found in the original sample are also identified in the NSP sample for both systems VBM-2/CaCl₂ and VBM-2/CaCl₂/CB. At 500 °C, the peak intensities of the LiNiO₂ phase decrease drastically for the VBM-2/CaCl₂. In the case of the VBM-2/CaCl₂/CB system, the phase LiNiO₂ is

no longer detected; instead, NiO and CaCO₃ are detected as reaction products. Therefore, we can infer that at 500 °C, LiNiO₂ starts to react with CaCl₂. When the temperature is increased to 700 °C, NiO and CaCO₃ are the reaction products for the VBM-2/CaCl₂ system. Whereas metallic Ni, CaCO₃, and NiO are identified as reaction products for the VBM-2/CaCl₂/CB system. The peaks of the NiO phase are largely reduced in intensity.

Concerning SBM, at 350 °C, the LiCoO₂ phase originally found in the cathode material is still present in the XRD pattern of the NSP sample for both systems SBM/CaCl₂ and SBM/CaCl₂/CB. At 500 °C, the peak intensities of the LiCoO₂ phase significantly decrease, the characteristic peaks of the CoO phase start to become noticeable, and only one peak corresponding to the CaCO₃ phase can be detected in the case of the SBM/CaCl₂ system. The characteristic peaks of the LiCoO₂ phase disappear completely, whereas the peaks of the CoO and CaCO₃ phases are well defined in the case of the SBM/CaCl₂/CB system. At 700 °C, the identified crystalline products are CoO and CaCO₃ for the SBM/CaCl₂/CB system. In addition to CoO and CaCO₃, characteristic peaks of metallic Co are also identified, indicating a superior reducing effect of the CB for the SBM/CaCl₂/CB system.

The graphite phase originally found in the black mass samples was also identified in all NSP samples. The comparative analysis of the XRD patterns of the NSP samples indicates that the original oxide present in the black mass sample is completely attacked at 700 °C for both studied systems.

Figure 5 exhibits the SEM micrographs and EDS spectra of NSP samples from the calcination of the BM/CaCl₂/CB sample at 700 °C. If we draw a comparison with the SEM micrographs from Figure 2, we can infer that the samples are attacked because they have very different morphology after the heat treatment. Regarding EDS results, the elements detected are as follows: C, O, Ni, Al, Ca, Mn, and Co in VBM-1; C, O, Ni, Al, Ca, and Co in VBM-2; and C, O, Ca, Mn, Co, and Ni in SBM. Considering the XRD results, the detection of Ca by EDS in the three NSP samples can be associated with the CaCO₃ phase.

In the case of VBM-1, the presence of C can be associated with the graphite phase detected by XRD. The presence of Ni can be associated with metallic Ni, while the presence of Mn can be associated with the MnO₂ phase. The presence of Al is due to the Al impurity identified in the original black mass sample. The presence of Co cannot be associated with any crystalline phase since Co-containing phases are not detected in the XRD pattern of the corresponding NSP sample.

Regarding VBM-2, the presence of C can also be associated with the graphite phase detected by XRD. The presence of Ni can be associated with the NiO phase and metallic Ni. The presence of Al is also due to the Al impurity detected in the original black mass sample. The presence of Co cannot be associated with any crystalline phase since Co-containing phases are not detected in the XRD pattern of the corresponding NSP sample.

With respect to SBM, the presence of C can be associated with the graphite phase detected by XRD. The presence of Co can be associated with the CoO phase and metallic Co. Neither the presence of Ni nor Mn can be associated with any crystalline phases since Co- and Mn-containing phases were not detected in the XRD pattern of the corresponding NSP sample. Ni and Mn from the original sample were detected by AAS.

Figure 6 shows the XRD patterns of the SP samples obtained after the isothermal experiment performed at 700 °C for the BM/CaCl₂/CB system. Figure 4a–c show the results of SBM, VBM-1, and VBM-2, respectively. All patterns exhibit characteristic diffraction maxima of LiCl and hydrated LiCl. Minor characteristic peaks of LiF were also detected; this result can be attributed to possible impurities associated with traces of electrolyte that may have still been present in the original black mass sample. The presence of LiF could also be due to the formation of a solid electrolyte interface (SEI) during the lithiation/delithiation process (i.e., lithium intercalation process).

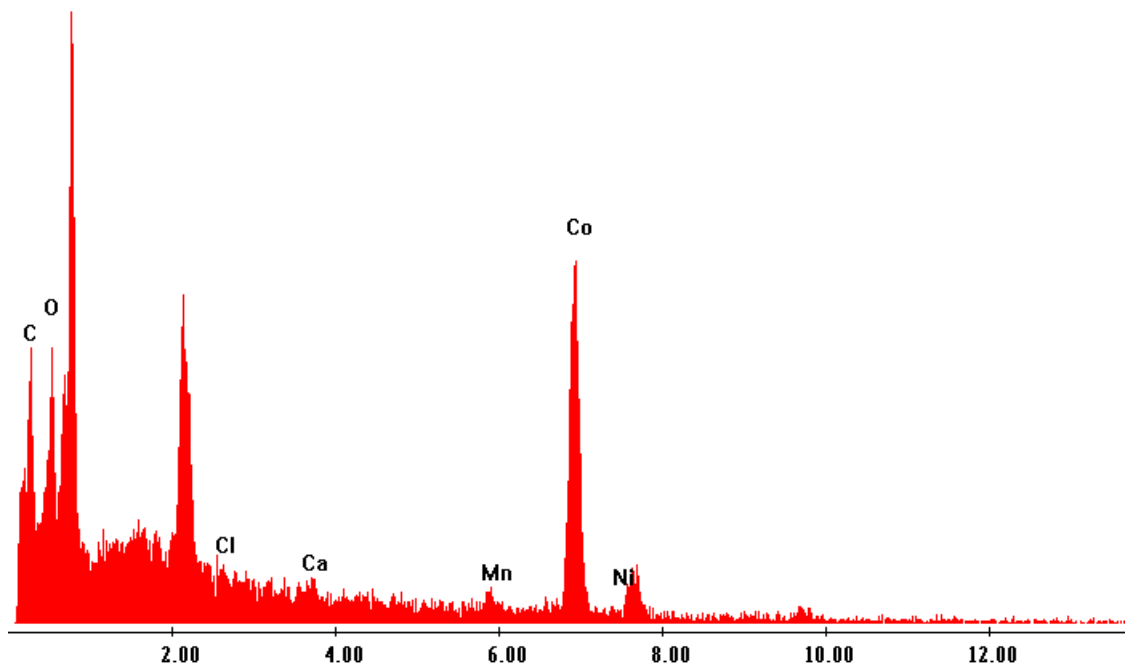
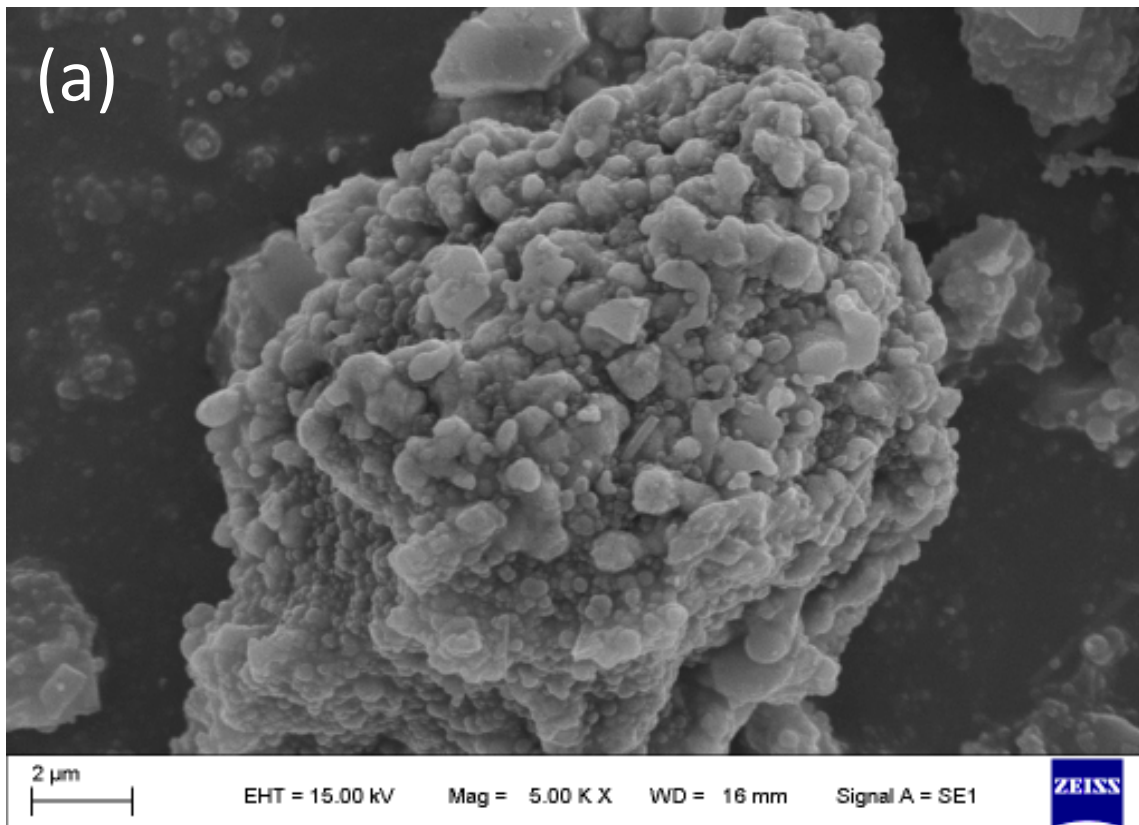


Figure 5. Cont.

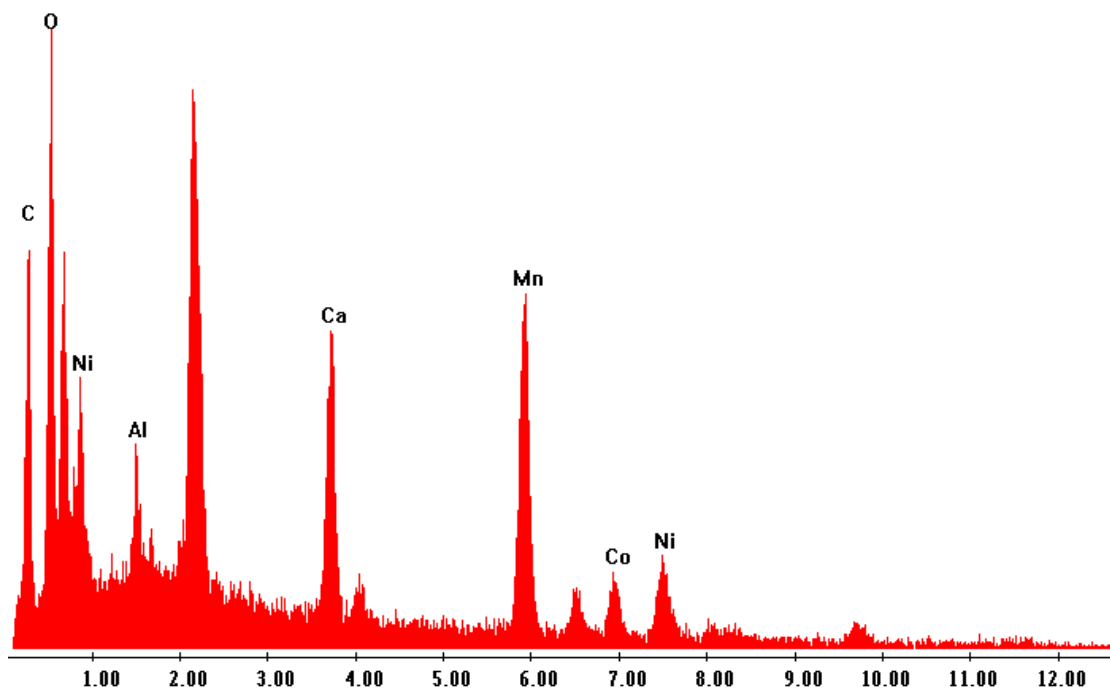
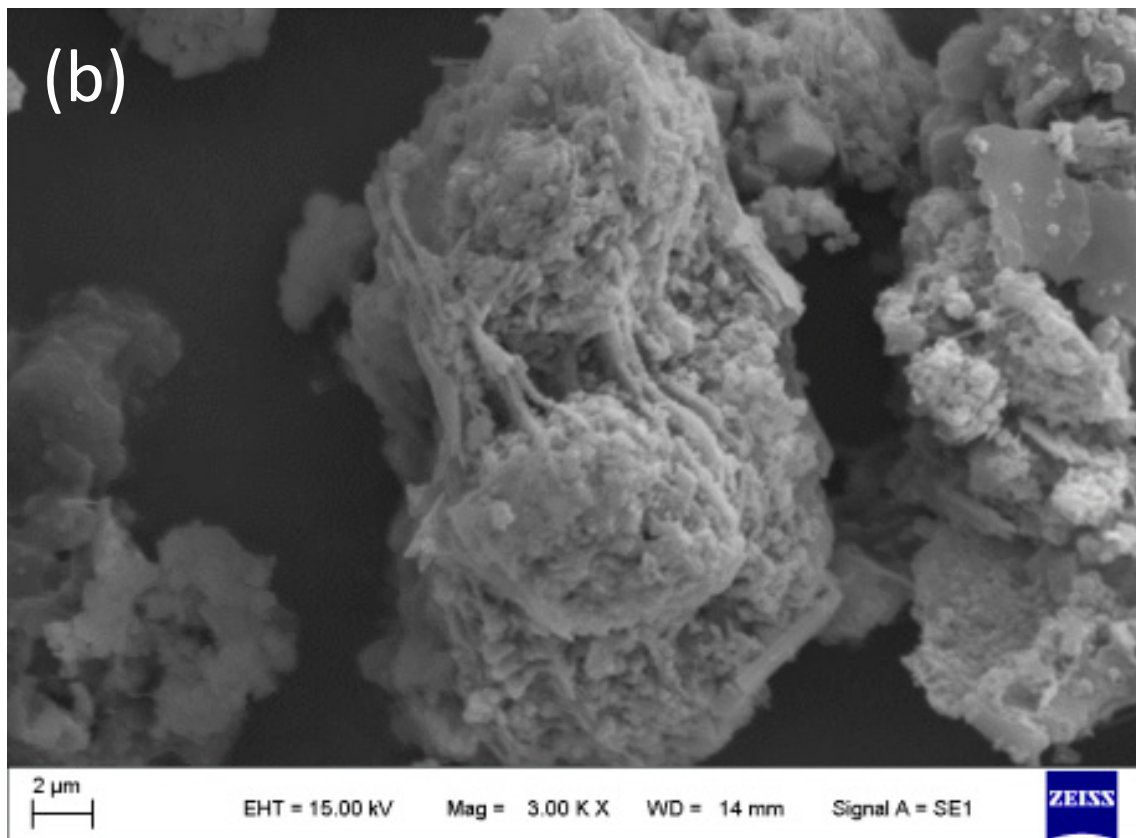


Figure 5. Cont.

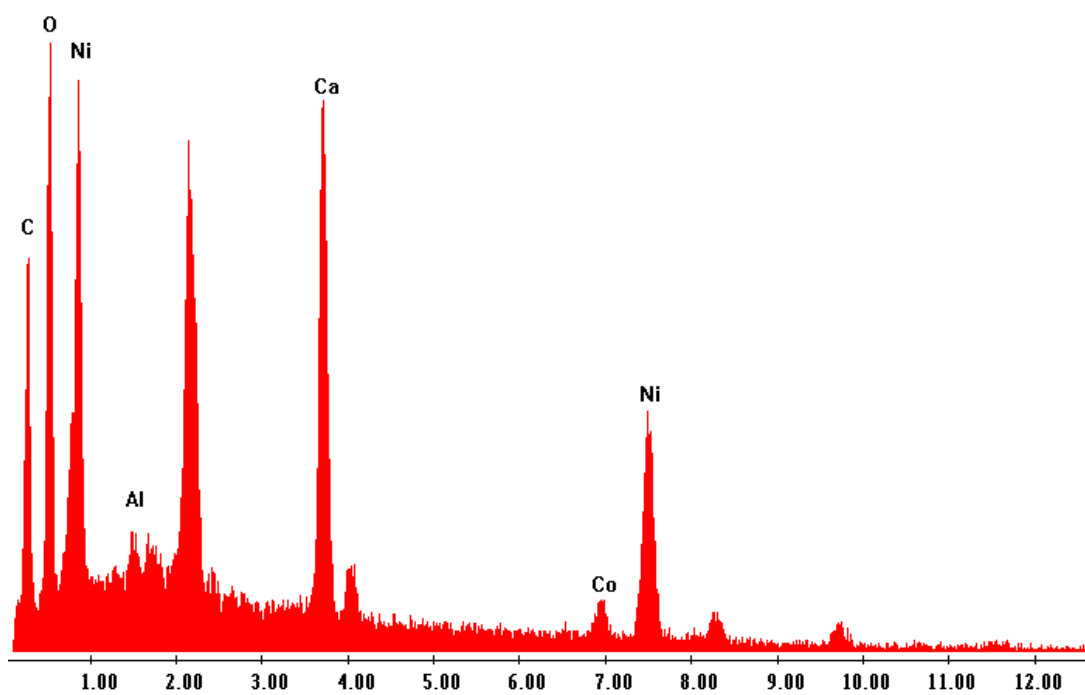
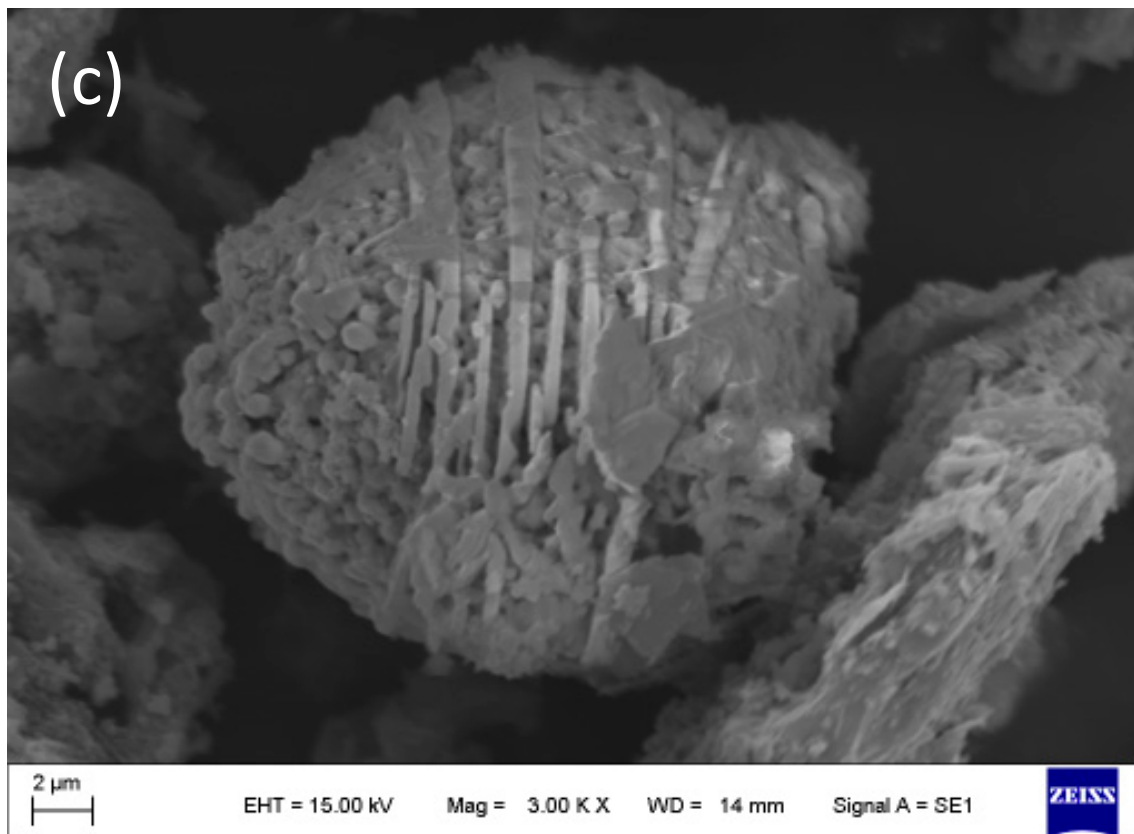


Figure 5. SEM micrographs and EDS spectra of NSP samples from the calcination of BM/CaCl₂/CB at 700 °C. (a) SBM, (b) VBM-1, and (c) VBM-2.

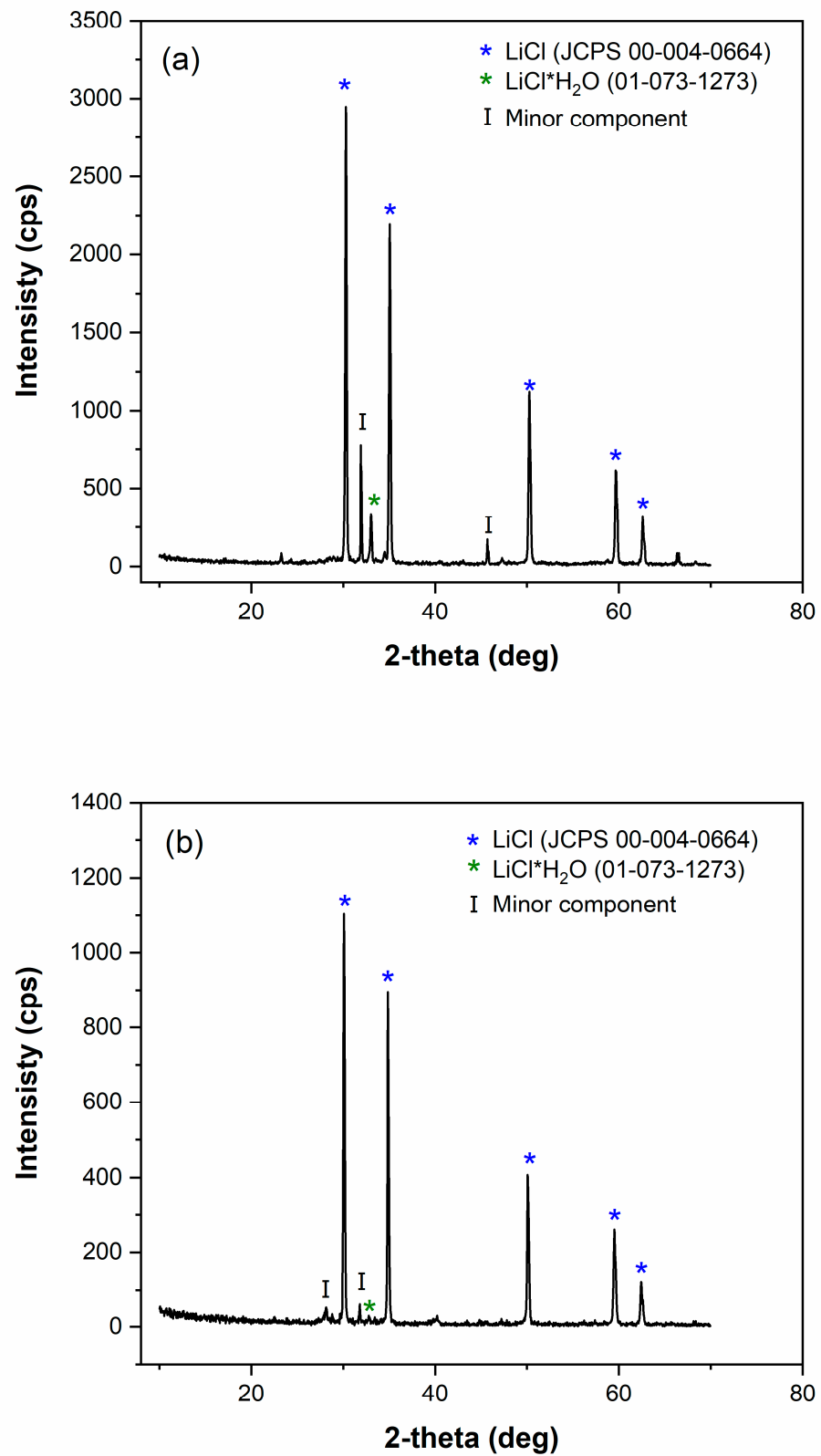


Figure 6. Cont.

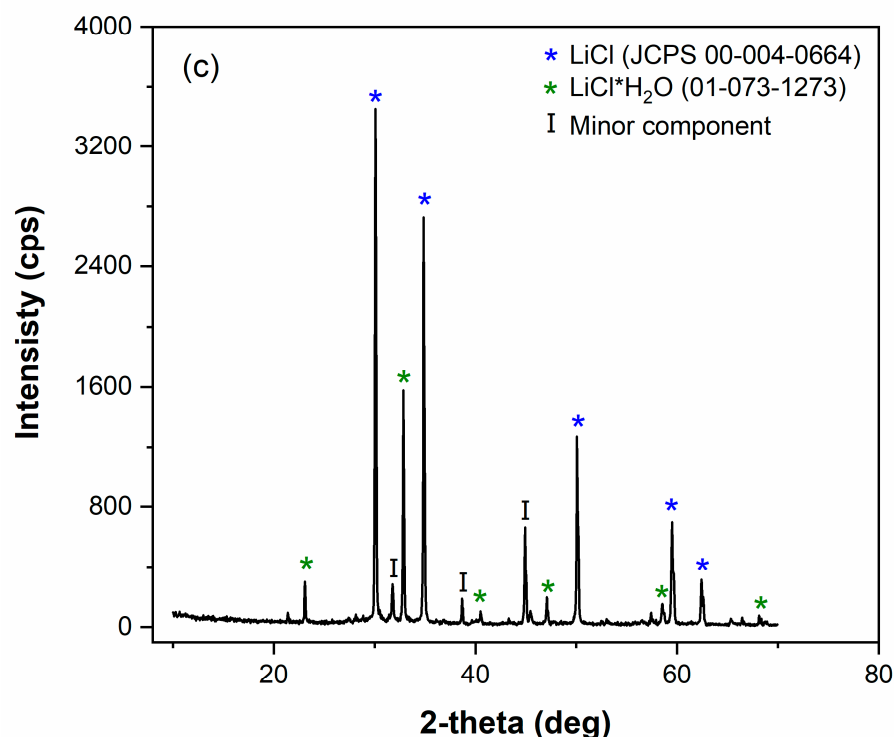


Figure 6. XRD patterns of the SP samples from the isothermal experiment at 700 °C for the BM/CaCl₂/CB system: (a) VBM-1, (b) VBM-2, and (c) SBM.

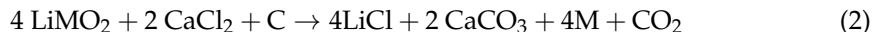
Figure 7 presents the SEM micrographs of the SP samples. The particles of the three samples have a microscopic structure with a high degree of crystallization, agglomeration, and approximate laminated morphology with a smooth surface and a hexagonal shape. Elemental analysis shows the presence of Cl. These results confirm that LiCl is predominantly present in the SP samples. Therefore, lithium is extracted selectively as LiCl from each black mass sample by the process of carbochlorination with CaCl₂. Other elements are detected in SP samples by EDS; they are impurities that originated during sample preparation.

Table 3 compares the lithium extraction results of both systems, BM/CaCl₂ and BM/CaCl₂/CB, from isothermal experiments performed at 500 and 700 °C. The lithium extraction values at 500 °C are higher than those obtained at 700 °C for both systems. A closer inspection of the table shows that the extraction levels from the BM/CaCl₂/CB combination are considerably higher than those obtained from the BM/CaCl₂ combination. Quantitative extraction is reached from the BM/CaCl₂/CB combination at 700 °C for the three samples. Overall, the extraction results agree with XRD results. With regard to the XRD results of the NSP samples, the levels of extraction agree well with either a significant decrease in the intensity peaks or complete disappearance of the original phase intensity peaks.

Table 3. Lithium extraction at 500 °C and 700 °C for 60 min.

Temperature (°C)	BM/CaCl ₂	X (%)	BM/CaCl ₂ /Carbon Black	X (%)
500	VBM-1	35	VBM-1	76
	VBM-2	35	VBM-2	80
	SBM	60	SBM	95
700	VBM-1	90	VBM-1	99
	VBM-2	90	VBM-2	99
	SBM	95	SBM	99

Together, all the results indicate that the carbochlorination of the LiMO_2 structure (with $M = \text{Co}, \text{Ni-Mn},$ and Ni) is feasible at 500 and 700 °C. The reaction leads to LiCl as the only chloride generated. The whole carbochlorination process can be represented by reaction Equation (2):



Lithium is extracted from the structure of the initial LiMO_2 phase by the chlorinating action of calcium chloride. The presence of the carbon material favors the formation of CaCO_3 . Additionally, carbon black induces the reduction of the transition metal M to form metallic M . Temperature has a significant influence on lithium extraction and the products that can be evolved. Lithium extraction values at 700 °C are much higher than those at 500 °C for both systems, BM/CaCl_2 and $\text{BM}/\text{CaCl}_2/\text{CB}$. In the case of VBM-1 carbochlorination, at 500 °C, the oxide $\text{NiO}_{0.75}\text{MnO}_{0.25}$ evolves, while the oxide $\text{NiO}_{0.75}\text{MnO}_{0.25}$ and metallic Ni evolves when the temperature is increased to 700 °C for the VBM-1/ CaCl_2 . At 500 °C, $\text{NiO}_{0.75}\text{MnO}_{0.25}$ and MnO_2 evolve, while MnO_2 and metallic Ni evolve when the temperature is increased to 700 °C for the VBM-1/ CaCl_2/CB system. In the case of VBM-2 carbochlorination, at 500 °C, no oxide evolves, while NiO evolves when the temperature is increased to 700 °C for the VBM-2/ CaCl_2 . At 500 °C, NiO evolves, while NiO and metallic Ni evolve when the temperature is increased to 700 °C for the VBM-2/ CaCl_2/CB system. In the case of SBM carbochlorination, at 500 °C, CoO evolves, while CoO and metallic Co evolve when the temperature is increased to 700 °C for the SBM/ CaCl_2/CB system.

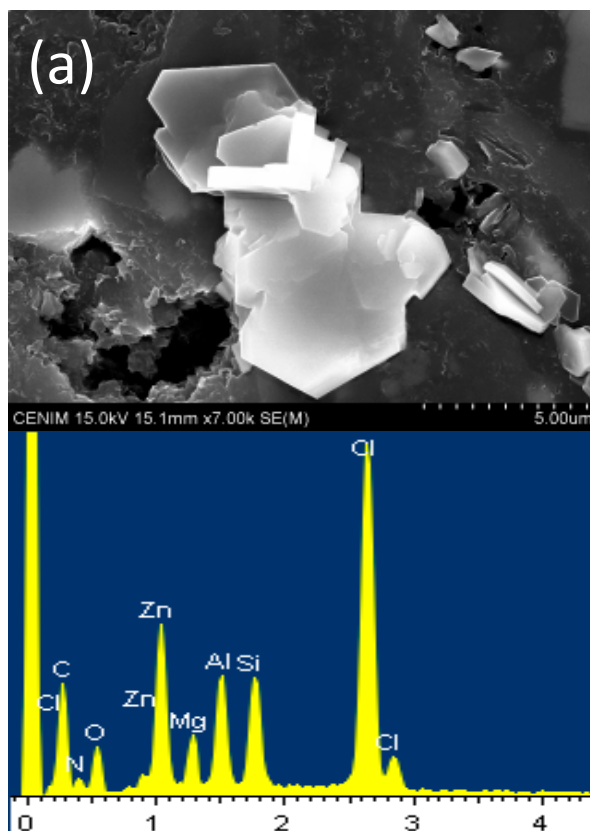


Figure 7. Cont.

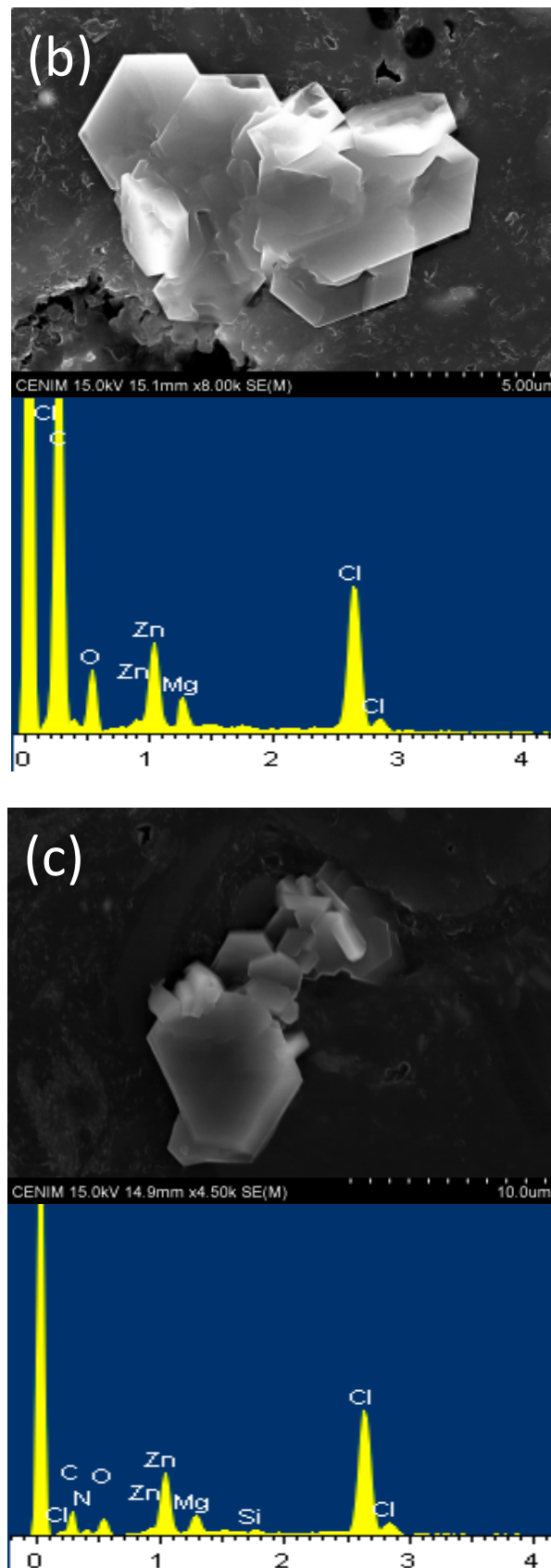


Figure 7. SEM micrographs and EDS spectra of the SP samples from the isothermal experiment at 700 °C for the BM/CaCl₂/CB system: (a) VBM-1, (b) VBM-2, and (c) SBM.

The presence of carbon black also has a great influence on lithium extraction and the reduction extent. Quantitative lithium extraction is achieved when carbon black takes part in the reaction system, while the maximum lithium extraction achieved is 95% when carbon black is not added to the system. The superior reduction action of carbon black is very notorious at 700 °C due to the presence of Ni and Co in their metallic state. However, the reduction from oxide to metal is not complete. Graphite, originally present in the black mass samples in high concentration, which in turn has a low reduction action as compared with carbon black [18,37], could be hindering the reduction reaction and preventing the complete reduction of Co and Ni to their elemental states. In addition, ash formed during the carbochlorination process may also be preventing the reaction of reduction of Co and Ni.

The present results are significant in at least two major respects. Lithium is selectively chlorinated using CaCl_2 as a chlorinating agent under the experimental conditions of this study. Then, LiCl can be easily recovered by water leaching. Another interesting finding is that the addition of carbon black favors the yielding of Co and Ni in their metallic state. Thus, both metals could be separated magnetically from CaCO_3 , another product of the carbochlorination reaction, and other impurities to fully recover the metals present in the black mass samples. Therefore, there is a need for further progress in determining the conditions and processes necessary to separate all metals from black mass samples with a high purity degree.

5. Conclusions

Carbochlorination using CaCl_2 as chlorinating agent and carbon black as reducing agent was an effective process to extract, selectively, lithium as lithium chloride from black mass samples with varied cathode chemistries from spent LIBs. Temperature and carbon type were the variables that had the most marked effect on the carbochlorination process. The extraction of lithium increased with temperature and the use of carbon black as a reducing agent. Quantitative lithium extraction was achieved at 700 °C for 60 min in the presence of carbon black in the reaction system. In addition, this process allowed us to recover Co and Ni in their metallic state, and as metallic oxide, they could be separated magnetically after a second calcination process. Finally, the researched methodology reveals that it is possible to effectively separate and recover different metals from discarded LIBs of different natures, leading to materials that could be used in the production of new batteries, which in turn could promote a circular economy and sustainable development goals.

Author Contributions: Conceptualization, F.A.L., L.B. and J.G.; methodology, F.A.L. and J.G.; validation, Y.C.G., L.B. and L.A.; formal analysis, Y.C.G., L.A. and F.J.A.; investigation, Y.C.G. and L.A.; resources, F.A.L.; chemical analysis, F.J.A.; writing—original draft preparation, Y.C.G.; writing—review and editing, L.A., L.B., J.G. and F.A.L.; supervision, F.A.L. and J.G.; funding acquisition, F.A.L. All authors have read and agreed to the published version of the manuscript.

Funding: This work was funded by the European Union's Horizon 2020 research under grant agreement No 776851 (Car-E Service).

Data Availability Statement: Not applicable.

Acknowledgments: Work carried out as part of the activities of the CSIC Interdisciplinary Thematic Platform PTI Mobility 2030. The authors gratefully acknowledge the financial support of Consejo Nacional de Investigaciones Científicas y Técnicas CONICET (PUE 2017-071), Universidad Nacional de San Luis UNSL (PROICO 02-1420), Fondo para la Investigación Científica y Tecnológica FONCYT (PICT 2018-3878), and Fundación Carolina—SEGIB 2020-2021 for financing mobility for doctoral research. We acknowledge the support for the publication fee from the CSIC Open-Access Publication Support Initiative through its Unit of Information Resources for Research (URICI).

Conflicts of Interest: The authors declare no conflict of interest.

References

1. Mirza, M.; Abdulaziz, R.; Maskell, W.C.; Tan, C.; Shearing, P.R.; Brett, D.J.L. Recovery of Cobalt from Lithium-ion Batteries using Fluidised Cathode Molten Salt Electrolysis. *Electrochim. Acta* **2021**, *391*, 138846. [[CrossRef](#)]
2. Moazzam, P.; Boroumand, Y.; Rabiei, P.; Baghbaderani, S.S.; Mokarian, P.; Mohagheghian, F.; Mohammed, L.J.; Razmjou, A. Lithium bioleaching: An emerging approach for the recovery of Li from spent lithium ion batteries. *Chemosphere* **2021**, *277*, 130196. [[CrossRef](#)] [[PubMed](#)]
3. Mossali, E.; Picone, N.; Gentilini, L.; Rodriguez, O.; Pérez, J.M.; Colledani, M. Lithium-ion batteries towards circular economy: A literature review of opportunities and issues of recycling treatments. *J. Environ. Manag.* **2020**, *264*, 110500. [[CrossRef](#)] [[PubMed](#)]
4. Velázquez-Martínez, O.; Valio, J.; Santasalo-Aarnio, A.; Reuter, M.; Serna-Guerrero, R. A critical review of lithium-ion battery recycling processes from a circular economy perspective. *Batteries* **2019**, *5*, 68. [[CrossRef](#)]
5. Nasser, O.A.; Petranikova, M. Review of achieved purities after li-ion batteries hydrometallurgical treatment and impurities effects on the cathode performance. *Batteries* **2021**, *7*, 60. [[CrossRef](#)]
6. Alcaraz, L.; Díaz-Guerra, C.; Calbet, J.; López, M.L.; López, F.A. Obtaining and Characterization of Highly Crystalline Recycled Graphites from Different Types of Spent Batteries. *Materials* **2022**, *15*, 3246. [[CrossRef](#)]
7. Chandran, V.; Ghosh, A.; Patil, C.K.; Mohanavel, V.; Priya, A.K.; Rahim, R.; Madavan, R.; Muthuraman, U.; Karthick, A. Comprehensive review on recycling of spent lithium-ion batteries. *Mater. Today Proc.* **2021**, *47*, 167–180. [[CrossRef](#)]
8. Bankole, O.E.; Lei, L. Battery Recycling Technologies: Recycling Waste Lithium Ion Batteries with the Impact on the Environment In-View. *J. Environ. Ecol.* **2017**, *4*, 14. [[CrossRef](#)]
9. Magalini, F.; Kuehr, R.; Baldé, C.P. eWaste en América Latina. *GSMA Lat. Am.* **2015**, 1–38.
10. Romo, L.A.; López-Fernández, A.; García-Díaz, I.; Fernández, P.; Urbieto, A.; López, F.A. From spent alkaline batteries to $Zn_xMn_{3-x}O_4$ by a hydrometallurgical route: Synthesis and characterization. *RSC Adv.* **2018**, *8*, 33496–33505. [[CrossRef](#)]
11. Ji, Y.; Jafvert, C.T.; Zhao, F. Recovery of cathode materials from spent lithium-ion batteries using eutectic system of lithium compounds. *Resour. Conserv. Recycl.* **2021**, *170*, 105551. [[CrossRef](#)]
12. Barbosa, L.; Luna-Lama, F.; Peña, Y.G.; Caballero, A. Simple and Eco-Friendly Fabrication of Electrode Materials and Their Performance in High-Voltage Lithium-Ion Batteries. *ChemSusChem* **2020**, *13*, 838–849. [[CrossRef](#)] [[PubMed](#)]
13. Costa, C.M.; Barbosa, J.C.; Gonçalves, R.; Castro, H.; Del Campo, F.J.; Lanceros-Méndez, S. Recycling and environmental issues of lithium-ion batteries: Advances, challenges and opportunities. *Energy Storage Mater.* **2021**, *37*, 433–465. [[CrossRef](#)]
14. Zubi, G.; Dufo-lópez, R.; Carvalho, M.; Pasaoglu, G. The lithium-ion battery: State of the art and future perspectives. *Renew. Sustain. Energy Rev.* **2018**, *89*, 292–308. [[CrossRef](#)]
15. Choubey, P.K.; Kim, M.S.; Srivastava, R.R.; Lee, J.C.; Lee, J.Y. Advance review on the exploitation of the prominent energy-storage element: Lithium. Part I: From mineral and brine resources. *Miner. Eng.* **2016**, *89*, 119–137. [[CrossRef](#)]
16. Olivetti, E.A.; Ceder, G.; Gaustad, G.G.; Fu, X. Lithium-Ion Battery Supply Chain Considerations: Analysis of Potential Bottlenecks in Critical Metals. *Joule* **2017**, *1*, 229–243. [[CrossRef](#)]
17. Pagliaro, M.; Meneguzzo, F. Lithium battery reusing and recycling: A circular economy insight. *Heliyon* **2019**, *5*, e01866. [[CrossRef](#)]
18. González, Y.C.; Barrios, O.C.; González, J.A.; Barbosa, L.I. Study on the carboreduction of the cathode material present in spent LIBs to produce Li_2CO_3 and CoO . *Miner. Eng.* **2022**, *184*, 107665. [[CrossRef](#)]
19. Zhou, L.F.; Yang, D.; Du, T.; Gong, H.; Luo, W.B. The Current Process for the Recycling of Spent Lithium Ion Batteries. *Front. Chem.* **2020**, *8*, 1–7. [[CrossRef](#)]
20. Yang, H.; Deng, B.; Jing, X.; Li, W.; Wang, D. Direct recovery of degraded $LiCoO_2$ cathode material from spent lithium-ion batteries: Efficient impurity removal toward practical applications. *Waste Manag.* **2021**, *129*, 85–94. [[CrossRef](#)]
21. Guo, Y.; Li, F.; Zhu, H.; Li, G.; Huang, J.; He, W. Leaching lithium from the anode electrode materials of spent lithium-ion batteries by hydrochloric acid (HCl). *Waste Manag.* **2016**, *51*, 227–233. [[CrossRef](#)] [[PubMed](#)]
22. Pinna, E.G.; Ruiz, M.C.; Ojeda, M.W.; Rodriguez, M.H. Cathodes of spent Li-ion batteries: Dissolution with phosphoric acid and recovery of lithium and cobalt from leach liquors. *Hydrometallurgy* **2017**, *167*, 66–71. [[CrossRef](#)]
23. Jung, Y.; Yoo, B.; Park, S.; Kim, Y.; Son, S. Study on Roasting for Selective Lithium Leaching of Cathode Active Materials from Spent Lithium-Ion Batteries. *Metals* **2021**, *11*, 1336. [[CrossRef](#)]
24. Lei, S.; Zhang, Y.; Song, S.; Xu, R.; Sun, W.; Xu, S.; Yang, Y. Strengthening Valuable Metal Recovery from Spent Lithium-Ion Batteries by Environmentally Friendly Reductive Thermal Treatment and Electrochemical Leaching. *ACS Sustain. Chem. Eng.* **2021**, *9*, 7053–7062. [[CrossRef](#)]
25. Yue, Y.; Wei, S.; Yongjie, B.; Chenyang, Z.; Shaole, S.; Yuehua, H. Recovering Valuable Metals from Spent Lithium Ion Battery via a Combination of Reduction Thermal Treatment and Facile Acid Leaching. *ACS Sustain. Chem. Eng.* **2018**, *6*, 10445–10453. [[CrossRef](#)]
26. Hu, J.; Zhang, J.; Li, H.; Chen, Y.; Wang, C. A promising approach for the recovery of high value-added metals from spent lithium-ion batteries. *J. Power Sources* **2017**, *351*, 192–199. [[CrossRef](#)]
27. Barrios, O.C.; González, Y.C.; Barbosa, L.I.; Orosco, P. Chlorination roasting of the cathode material contained in spent lithium-ion batteries to recover lithium, manganese, nickel and cobalt. *Miner. Eng.* **2022**, *176*, 107321. [[CrossRef](#)]
28. Movahedian, A.; Raygan, S.; Pourabdoli, M. The chlorination kinetics of zirconium dioxide mixed with carbon black. *Thermochim. Acta* **2011**, *512*, 93–97. [[CrossRef](#)]

29. González, J.; Bohé, A.; Pasquevich, D.; Del, M. β -Ta₂O₅ carbochlorination with different types of carbon. *Can. Metall. Q.* **2002**, *41*, 29–40. [[CrossRef](#)]
30. Banik, R.; Suresh, N.; Mandre, N.R. Selective Flocculation as a Pre-Concentration Process—An Overview. *Miner. Process. Extr. Metall. Rev. Int. J.* **1995**, *14*, 169–177. [[CrossRef](#)]
31. Barbosa, L.I.; González, J.A.; Ruiz, M.D.C. Extraction of lithium from β -spodumene using chlorination roasting with calcium chloride. *Thermochim. Acta* **2015**, *605*, 63–67. [[CrossRef](#)]
32. Qu, X.; Xie, H.; Chen, X.; Tang, Y.; Zhang, B.; Xing, P.; Yin, H. Recovery of LiCoO₂ from Spent Lithium-Ion Batteries through a Low-Temperature Ammonium Chloride Roasting Approach: Thermodynamics and Reaction Mechanisms. *ACS Sustain. Chem. Eng.* **2020**, *8*, 6524–6532. [[CrossRef](#)]
33. Jian, Y.; Zongliang, Z.; Gang, Z.; Liangxing, J.; Fangyang, L.; Ming, J.; Yanqing, L. Process study of chloride roasting and water leaching for the extraction of valuable metals from spent lithium-ion batteries. *Hydrometallurgy* **2021**, *203*, 105638. [[CrossRef](#)]
34. Li, W.; Song, B.; Manthiram, A. High-voltage positive electrode materials for lithium-ion batteries. *Chem. Soc. Rev.* **2017**, *46*, 3006–3059. [[CrossRef](#)]
35. Túnez, F.M.; González, J.; Ruiz, M.D.C. Aparato de Laboratorio para Realizar Termogravimetrías en Atmósferas Corrosivas y no Corrosivas. AR Patent 053676 A1, P060100450, 2007.
36. Zhao, B.L.; Li, N.; Langner, A.; Steinhart, M.; Tan, T.Y.; Pippel, E.; Hofmeister, H.; Tu, K.; Gösele, U. Crystallization of Amorphous SiO₂ Microtubes Catalyzed by Lithium. *Adv. Funct. Mater.* **2007**, *17*, 1952–1957. [[CrossRef](#)]
37. González, J.; Del Ruiz, M.C.; Bohé, A.; Pasquevich, D. Oxidation of carbons in the presence of chlorine. *Carbon N. Y.* **1999**, *37*, 1979–1988. [[CrossRef](#)]

Disclaimer/Publisher's Note: The statements, opinions and data contained in all publications are solely those of the individual author(s) and contributor(s) and not of MDPI and/or the editor(s). MDPI and/or the editor(s) disclaim responsibility for any injury to people or property resulting from any ideas, methods, instructions or products referred to in the content.